From: MOLECULAR IONS
Edited by Joseph Berkowitz and Karl-Ontjes Groeneveld
(Plenum Publishing Corporation, 1983)

STRUCTURES OF MOLECULAR IONS FROM LASER MAGNETIC RESONANCE SPECTROSCOPY

Richard J. Saykally and Karen G. Lubic

Department of Chemistry
The University of California
Berkeley, California

and

Kenneth M. Evenson

National Bureau of Standards
Boulder, Colorado 80302

INTRODUCTION

The status of molecular ion spectroscopy was elegantly reviewed by Dr. G. H. Herzberg in his Faraday Lecture to the Chemical Society [1] in September of 1971. As of that time thirty-three diatomic ions and six polyatomic ions had been studied by spectroscopic methods. All of these had been observed by absorption or emission in the visible region of the spectrum, except for H_2^+; it had become the first molecular ion to be detected by a high resolution (better than the optical Doppler width) technique in 1968 through the work of K. B. Jefferts [2].

The last decade has witnessed dramatic advances in the spectroscopy of molecular ions. The HCO^+ [3] and HNN^+ [4] ions have been established as important and ubiquitous constituents of interstellar clouds by the powerful new radio astronomy techniques that have been used to detect them. Microwave spectroscopy has been successful in detection of rotational spectra and the determination of precise structures for CO^+ [5], HCO^+ [6], and HNN^+ [7]. Ion beam spectroscopy has produced vibrational spectra of HD^+ [8], HeH^+ [9], and D_3^+ [10] and high resolution electronic spectra of CO^+ [11], H_2O^+ [12], O_2^+ [13,14], and HD^+ [15]. Far infrared laser magnetic resonance spectroscopy has been used to detect pure rotational spectra of HBr^+ [16]. Most recently, vibrational

absorption spectra of H_3^+ have been detected with a tunable infrared difference frequency laser system [17]. In addition, optical spectra have been observed for a number of molecular ions stored in radiofrequency traps by laser induced fluorescence [18].

As of this date spectra of over 60 different molecular ions have been detected. Nine of these ions have been studied with high resolution methods. In this paper we will discuss the use of one of these promising new techniques -- far-infrared laser magnetic resonance -- to obtain detailed information on the geometrical and electronic structures of molecular ions. We begin by reviewing the general principles of LMR and describing the experimental design.

THE LASER MAGNETIC RESONANCE EXPERIMENT

LMR [19] is very closely related to the technique of gas-phase electron paramagnetic resonance developed by Radford and by Carrington and his collaborators over a decade ago. In both experiments the paramagnetic energy levels of an atom or molecule contained in a resonant cavity are tuned by a dc magnetic field until their energy difference matches that of a fixed frequency source. The final product of the spectrometers is then an absorption spectrum as a function of magnetic flux density. The principal distinction between the two experiments is that EPR transitions are usually between different magnetic sublevels (M_J) of a particular angular momentum state (J), whereas the LMR transitions occur between different rotational states. The laser magnetic resonance experiment therefore has the prerequisite that a given transition frequency must lie very close (within 1% on the average) to a far-infrared lasing transition. It was this requirement that severely constrained the applicability of LMR during the first decade of its inception, since only a few laser lines were then available from the H_2O and HCN gas lasers that were used as sources. The optically-pumped far-infrared laser has now dramatically expanded the scope of LMR, providing a discretely tunable source covering most of the far-infrared (50-1000 μm).

LMR derives its power from the really remarkable combination of sensitivity and resolution it can produce. Using the OH radical for comparison, it has been found that EPR can detect a density of about 2×10^{10} cm^{-3}, while microwave spectroscopy is at least an order of magnitude less sensitive. Resonance fluorescence methods (with a water vapor discharge source) can detect near 3×10^9 cm^{-3}. With laser magnetic resonance we can detect an OH density of 5×10^5 cm^{-3}. The only technique presently more sensitive is laser induced fluorescence, with a proven detection limit of 1×10^6 cm^{-3} in ambient air, but certainly much less with optimum conditions. This method, however, is limited in resolution by the optical

Doppler width ($\sim$1 GHz on the average), while LMR produces a collision-broadening linewidth of about 10 MHz at normal operating pressures (1 torr), and an easily accessible Doppler width of about 1 MHz. Sub-Doppler resolution can often be effected by using saturation dip techniques because the sample is located inside the optical cavity of the laser. Therefore, LMR can give us essentially the resolution of a microwave spectroscopy experiment with up to a million times the sensitivity!

A schematic diagram of the optically pumped LMR spectrometer built at the National Bureau of Standards in Boulder, Colorado is given in Figure 1. A gas (e.g., CH_3OH) having a strong vibrational absorption line that coincides with a CO_2 laser frequency is pumped nearly transversely by a CW, grating and piezoelectrically tuned CO_2 laser operating on a single mode with powers of up to 50 watts. The far-infrared lasing action is induced between rotational states of the upper vibrational level and oscillates inside the cavity defined by one fixed mirror and another mounted on a micrometer drive. The cavity mode spacing ($c/2\ell$ = 150 MHz) is much larger than the gain profile (5 MHz), so the laser length can be adjusted to select a single longitudinal mode, while higher order transverse modes are extinguished with an iris diaphragm. A piece of 13μm thick polypropylene stretched on a mount at the Brewster angle separates the transversely-pumped gain cell from the sample region of the cavity. This polarizes the laser radiation, and the polarization can then be rotated to select either σ or π orientation relative to the magnetic field. The sample region of the cavity is located between the pole faces of a 15" electromagnet, operating with 15 cm pole tips and a 7.2 cm airgap. Maximum fields of 20 kG can be obtained with this configuration.

The total power oscillating inside the cavity is monitored by coupling a small fraction of it out of a polyethylene window with a 4 mm diameter copper mirror machine at 45° which is mounted on a small rod. This coupling mirror can be inserted into the laser mode pattern to optimize the output coupling for each laser line. A liquid helium cooled gallium-doped germanium bolometer which has a NEP of about 6×10^{-12} $WHz^{-1/2}$ is used to detect the coupled radiation. An ac magnetic field of up to 50 G is produced by a set of Helmholtz coils operating at 1kHz, and lock-in detection is used to process the signals. The LMR spectrometer operates within an order of magnitude of the quantum noise limit set by the laser, about 1.4×10^{-12} watts. The minimum detectable one-way intracavity loss has been shown to be about 2×10^{-10}; this is roughly 1000 times less than could be achieved with a single pass through an external cell. After normalizing with the effective path length inside the cavity (about 75 cm, determined by the flame extent and the finesse of the cavity) we find that the direct interaction between the absorbing intracavity sample and the laser gain medium produces an enhancement in the sensitivity of about a

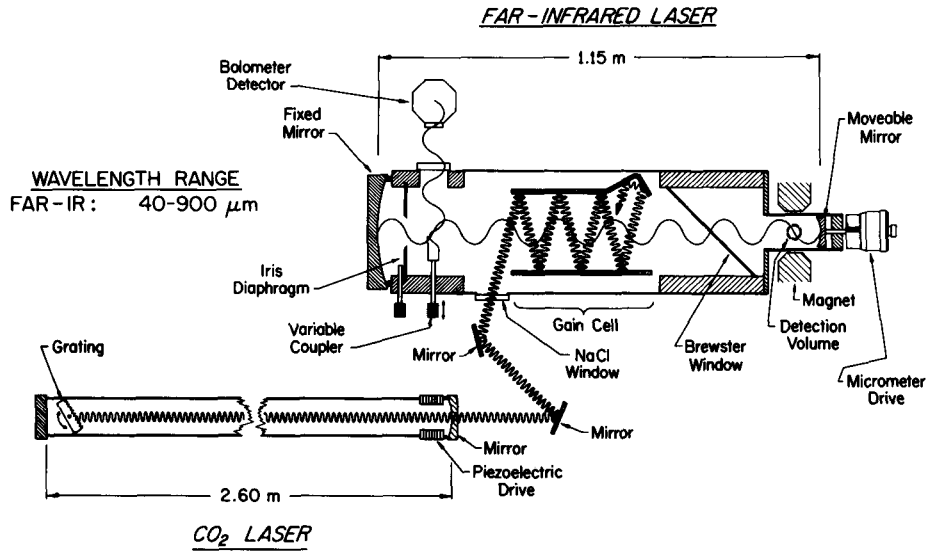

Fig. 1. Schematic diagram of an optically pumped far infrared LMR spectrometer.

factor of 20.

All of the free radicals observed until 1978 were generated in low pressure (1 Torr) flames burning inside the laser cavity. The methane fluorine atom reaction has been a particularly affluent souce of radicals. Evenson and his co-workers have now observed CH, CH_2, CCH, CH_2F, CF, CF_2, and C atoms in this one flame alone [19]. By modifying the laser design to accommodate an intracavity positive column discharge and incorporating a solenoid magnet to provide the field, we were able to detect the LMR spectra of metastable states of CO and O_2, the O atom, and the HBr^+ molecular ion. These experiments will be discussed in the next section.

LASER MAGNETIC RESONANCE DETECTION OF A MOLECULAR ION

The discharge LMR spectrometer consists of a 7.6 cm diameter by 38 cm long quartz far-infrared gain cell pumped transversely by a 2.3 meter CO_2 laser with a 30 watt single line output. The pumping geometry and output coupling is otherwise identical to that in Figure 1. The gain cell is separated from the 5 cm diameter by 58 cm long sample region by a 13 μm beamsplitter. Instead of being located inside the pole faces of a 15" transverse magnet, the sample region is centered inside the bore of a 5 cm diameter by 33 cam long solenoid magnet cooled by liquid nitrogen. The magnet can produce fields of 6 kG with a homogeneity of 0.1% over a

15 cm length. An ac modulation field was provided by a solenoidal coil wound to be concentric with the liquid nitrogen-cooled magnet. Since the solenoid produces an axial magnetic field, only σ-type transitions can be observed with this system. A dc glow discharge is maintained between a water-cooled copper cathode located in a sidearm outside of the optical cavity and a cylindrical copper anode located about 3 cm from the beamsplitter. Magnetic field measurements are made by placing a calibrated shunt resistor (0.01 Ω) in series with the magnet, keeping it at a constant temperature in a thermostated oil bath, and measuring the voltage drop across it with a digital voltmeter. The relationship between voltage and magnetic field in the sample region is calibrated with a NMR gaussmeter, and was determined to be linear over the entire range of fields available. With this system, flux densities can easily be measured with a precision of about 0.5 G.

The vacuum for the sample region is provided by a 750 l/min mechanical pump. Generally the discharge is operated at about 1 Torr total pressure with a fairly slow flow rate (~100 l/min). Pressures in both the sample region and gain cell are monitored with capacitance manometers.

The plasma is generally run at relatively low currents (<50 mA). The plasma density at zero magnetic field is in the range 10^8–10^{10} cm^{-3}. With an axial magnetic field one can expect the plasma density to increase markedly because the ambipolar diffusion of the electrons and ions to the walls is inhibited. We have, in fact, observed this effect in some of our spectra. In discharges of this nature, one generally observes a high electron temperature (20,000°K) while the translational and rotational degrees of freedom of molecules in the plasma are nearly thermalized at the wall temperature. Because vibrational relaxation is so much slower, vibrational temperatures can often exceed several thousand degrees.

The electric field in the positive column plasma filling the laser cavity is a few volts/cm. As a consequence, the positive ions will experience a net drift velocity of a few hundred meters per second toward the cathode in addition to their predominant radial motion. In the microwave studies of ions at the University of Wisconsin [5-7], this drift velocity was measured by virtue of the resulting Doppler shift of about 100 kilohertz in the microwave absorption frequency. In the LMR experiment the plasma is sampled by a standing wave rather than a traveling wave; therefore the slow drift velocity will manifest itself as a broadening of the absorption lines rather than a frequency shift.

The presence of the plasma causes a definite shift in the resonant frequency of the cavity, as expected from its higher refractive index. In principle, this shift could provide a direct

measurement of the plasma density. The plasma also introduces high frequency noise into the lock-in-detection system. One of the major experimental problems is simply to minimize this plasma noise, which is done empirically by varying pressure, current, and gas composition.

The first experiments performed with this glow discharge apparatus consisted of detecting spectra of OH and O_2 in the plasma. The $J = 1 \rightarrow 2$ fine structure transition in atomic oxygen was then found at 63. 1 μm, using $^{13}CH_3OH$ as the lasing medium. The measured fine structure splitting was determined to be 158.3098(7) cm^{-1} using precise g-factors from earlier EPR studies. The O atoms were produced in a discharge through a 1% mixture of O_2 in He. The signal intensity was found to be proportional to the current over the range 0-100mA and was roughly independent of the total pressure. The transition is shown in Figure 2 [20].

The $J = 8 \rightarrow 9$ rotational transition of the $a^1\Delta_g$ state of O_2 was found next, using the 392 μm laser line of CH_3OH in a discharge through pure O_2. This spectrum is particularly interesting because it demonstrated the capability of this spectrometer to produce sub-Doppler saturation dip spectra, as exhibited in Figure 3. It was analyzed along with several others observed for the $a^1\Delta_g$ state in the conventional LMR apparatus, using the afterglow of a 2450 MHz discharge as the source of metastables. The results of this work

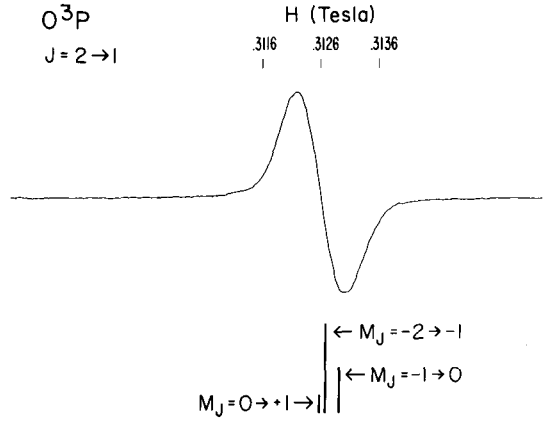

Fig. 2. The $J = 2 \rightarrow 1$ transitions of O (2^3P). The line shape for these transitions, observed in a 40 mA glow discharge through a mixture of ∿2% O_2 in helium at 133 Pa total pressure with the 63.1 μm laser line of $^{13}CH_3OH$ pumped by the 10.3 μm P(12) line of a CO_2 laser, is shown along with the calculated positions and intensities of the individual m-components.

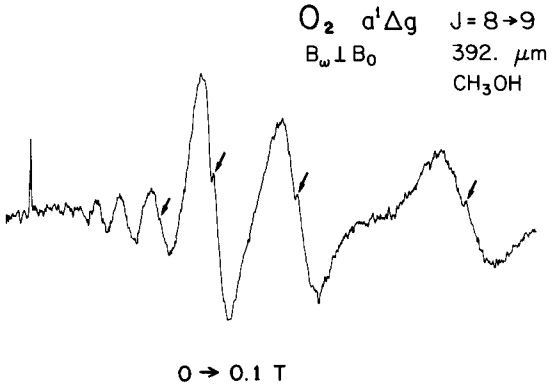

Fig. 3. Laser magnetic resonance spectrum of the J = 8 → 9 transition of $a^1\Delta_g$ O_2 observed with the 392.1 μm line of CH_3OH. Saturation dips are marked with arrows.

will be published shortly [21].

Another interesting result was the detection of pure rotational spectra of the metastable $a^3\Pi$ state of CO [22]. This state is quite short-lived, with a radiative lifetime of about 7.5 msec. These results are being analyzed along with earlier molecular beam and microwave data [23] in an attempt to obtain a more reliable set of molecular parameters for this state.

Of course, all of these experiments were done as "tune-ups" for the ultimate experiment -- a search for the spectrum of a molecular ion! A consideration of the possible candidates for this initial experiment revealed HCl^+ as being the best suited. It had been carefully studied by optical spectroscopy [24] and its rotational transitions could be predicted accurately. Its discharge kinetics had been the subject of flowing afterglow experiments [25] and it could be expected to be an abundant ion in a discharge through a dilute mixture of HCl in He. And it had a reasonably close coincidence between a low-J rotational transition and a known laser line. However, a series of intense searches for the spectrum of HCl^+ failed, for reasons which are not yet totally clear. We decided to try the experiment on the analogous HBr^+ ion.

The search was based on predictions of rotational transition frequencies from the optical work of Barrow and Caunt [26]. An energy level diagram of the $^2\Pi$ ground state calculated from their results is given in Figure 4. A discharge through a few percent of HBr in helium at about 1 torr was used to generate the ion. After considerable effort, a spectrum which could quite definitively be attributed to HBr^+ was observed. This was the J = 3/2 → 5/2

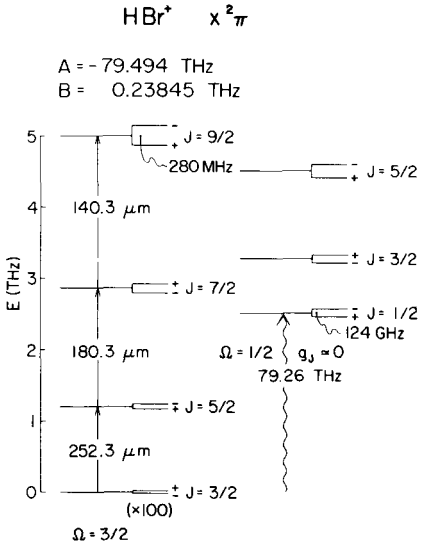

Fig. 4. Energy level diagram for the $^2\Pi$ ground state of HBr^+. The small lambda doubling in the $\Omega = 3/2$ state (Case A notation) is multiplied by 100; that in the diamagnetic $\Omega = 1/2$ state is to scale. The molecular parameters used to calculate the energies are taken from Ref. 26.

transition in the $\Omega = 3/2$ ground state, shown in Figure 5.

The maximum signal-to-noise ratio was obtained with a current of 15 mA and 1 torr of a 1% mixture of HBr in helium. An increase in the HBr content beyond a few percent caused the lines to disappear. Similarly, the addition of small amounts of air, O_2, H_2, or H_2O to the discharge resulted in large decreases in the signal. When HBr was replaced by DBr the spectra could not be obtained.

The strongest evidence that the spectrum was due to HBr^+ is provided by spectroscopic considerations. The transition was found very near the resonant field predicted from optical data. Because there are two equally abundant bromine isotopes (masses 79 and 81) each having a nuclear spin of 3/2, one expects to observe two sets of quartets for every M_J transition, with each line split by the lambda doubling. This is exactly the pattern that was found. Because we could only reach fields of 5 kG at this time, only the fastest tuning Zeeman component could be observed ($J = -3/2 \rightarrow -1/2$). By shifting the laser frequency ($d\nu$) and observing the shift in magnetic field (dH) we determined the sign of the tuning rate $dH/d\nu$, which told us that the laser frequency was above the zero field transition frequency, as predicted.

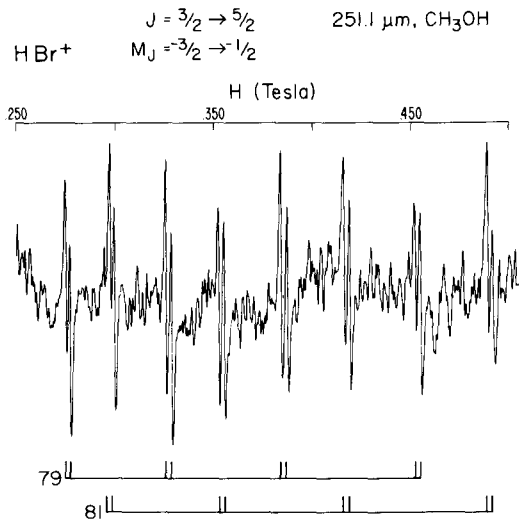

Fig. 5. The laser magnetic resonance spectrum of the J = 3/2 → 5/2 transition of HBr^+ observed at 251.1 μm (CH_3OH). This spectrum was recorded on a single scan with a 0.1 sec time constant in a glow discharge through 1% HBr in helium at a pressure of 133 Pa (1 torr). The positions of the eight doublets represent the hyperfine splitting in the M_J = -3/2 → -1/2 Zeeman transition. The doublet splitting is due to the lambda doubling.

With this degree of assurance as to the identity of the carrier, we searched for and easily found the J = 5/2 → 7/2 transition with the 180.7 μm line of CD_3OH, as shown in Figure 6. Again, the spectral features were much as predicted. The chemistry tests were repeated as before with the same results. Then the J = 3/2 → 5/2 transition was detected with a different laser line, the 253.7 μm line of CH_3OH. The J = 3/2 → 5/2 transition of DBr^+, predicted by scaling the hydrogen isotope constants for reduced mass was then found. Finally, the J = 5/2 → 7/2 transition of HBr^+ in the v = 1 state was detected just where it was predicted to be. Several other strong laser lines were used to check for spurious transitions, with negative results.

In subsequent experiments, the maximum field of the magnet was extended out to 6.2 kG. The spectra were then taken over the entire range of fields, and the next M_J components of all of the transitions were found. Magnetic flux densities were measured for the three v = 0 HBr^+ spectra with accuracies of ±1 kG, using the digital voltmeter scheme described earlier. Attempts were made to detect an increase in the linewidth by operating the discharge

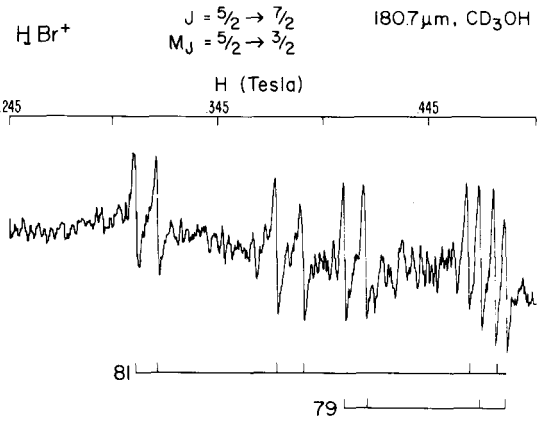

Fig. 6. The J = 5/2 → 7/2 transition of HBr^+ observed at 180.7 μm (CD_3OH) under the same conditions used in Figure 2. Only the first eight hyperfine lines of the M_J = 5/2 → 3/2 Zeeman component could be reached with available magnetic fields.

in an abnormal glow mode with a higher voltage drop but these experiments predictably failed. As can be seen in Figure 5, the intensity of the otherwise equally intense hyperfine components shows a small but definite increase as the field is increased.

ASSIGNMENT AND ANALYSIS OF THE SPECTRUM

As with all spectroscopic techniques, there is good news and bad news about laser magnetic resonance. The good news is the tremendous sensitivity and high resolution that can be obtained, and the fact that about 90% of the features of a LMR spectrum for a "nice" molecule (one that does not exhibit Paschen-Bach effects) can be predicted, explained, and understood in terms of very simple first-order expressions. The bad news pertains to the remaining 10% that cannot. It becomes very laborious, time-consuming, and expensive to correctly account for it. LMR produces data that are among the most difficult molecular spectra to analyze accurately. In this section we will discuss the problem of assignment and analysis of the LMR spectrum of HBr^+.

The Zeeman energy of a paramagnetic atom or molecule can be expressed to first-order as

$$E = E_0 + \mu_0 Hg_J M_J \qquad (1)$$

where E_0 is the zero-field energy, μ_0 is the Bohr magneton, H is

the magnetic flux density, g_J is an effective g-factor for the angular momentum state J, and M_J is the space projection of J. For a $\Delta M_J = 0$ transition between states E' (upper) and E" (lower) we obtain

$$\nu_L = \nu_0 + \mu_0 H(g' - g'') M_J'' \tag{2}$$

where $\nu_0 = E_0' - E_0''$ and $\nu_L = E' - E''$ is the frequency difference which must match the laser frequency at resonance. For $\Delta M_J = \pm 1$ transitions we get

$$\nu_L = \nu_0 + \mu_0 H(g' - g'') M_J'' \pm \mu_0 Hg' \tag{3}$$

The magnetic tuning rates of these transition frequencies are

$$\frac{\partial \nu_L}{\partial H} = \nu_0(g' - g'') M_J'' \qquad \Delta M_J = 0$$

$$= \mu_0(g' - g'') M_J'' \pm \mu_0 g' \qquad \Delta M_J = \pm 1 \tag{4}$$

Solving (2) and (3) for the resonant magnetic fields we obtain

$$H = \frac{\nu_L - \nu_0}{\mu_0(g' - g'') M_J''} \qquad \Delta M_J = 0$$

$$H = \frac{\nu_L - \nu_0}{\mu_0(g' - g'') M_J'' \pm \mu_0 g'} \qquad \Delta M_J = \pm 1 \tag{5}$$

If we plot the reciprocal of the resonant fields versus M_J'', we obtain a straight line in each case with a slope of

$$\frac{\partial(1/H)}{\partial M_J''} = \frac{\mu_0(g' - g'')}{\nu_L - \nu_0}$$

For a $\Delta M_J = 0$ transition the intercept is zero, but for a $\Delta M_J = \pm 1$ transition it has the value

$$\frac{\mu_0 g'}{\nu_L - \nu_0}$$

These plots are very useful in initially assigning a LMR spectrum.

Another very useful tool for the assignment of a spectrum is

the "laser pulling" experiment. The reciprocal of the tuning rate given by (4) determines which direction the resonant field will shift if the laser frequency is shifted to the red or blue. If the sign of the term g' - g" is known (as it usually is), this will tell us the sign of M_J" and thus whether the laser frequency is above or below the zero-field transition frequency.

Specializing to the present case of a $^2\Pi$ molecule described by Hund's Case A, we note that the effective g-factor for a given J state is given by the vector model as

$$g_J = \frac{(\Lambda + 2.002\Sigma)\ \Omega}{J(J+1)} \tag{6}$$

Therefore g' - g" will always be negative for pure rotational transitions between the $\Omega = 3/2$ levels. This tells us that the fastest tuning Zeeman transition will be that with the largest negative M_J value if $\nu_L > \nu_0$ or the largest positive M_J if $\nu_L < \nu_0$. For a $\Delta M_J = \pm 1$ transition, we see from (5) that the fastest tuning transition will also be that with $\Delta M_J = +1$ if $\nu_L > \nu_0$ or $\Delta M_J = -1$ if $\nu_L < \nu_0$. In both of these last cases, the opposite branch ($\Delta M_J = -1$ if $\nu_L > \nu_0$ or $\Delta M_J = +1$ if $\nu_L < \nu_0$) will occur at higher fields. The relative intensities for all of these transitions are easily obtained from standard matrix elements of the direction cosine operator. With equations (1) through (6) and the direction cosine results the main features of the LMR spectrum can be predicted very easily.

Hyperfine interactions in LMR spectra are usually described at all but the lowest fields (<1 kG) by a decoupled representation, i.e., with nuclear spin independently quantized in the space-fixed axis system defined by the magnetic field. Therefore the effect of a nuclear spin I will be to split each Zeeman transition into 2I + 1 equally intense components. In a Case A molecule, the magnetic hyperfine energy can be expressed as simply

$$E_{MHf} = a_J\ M_I\ M_J \tag{7}$$

where a_J is an effective hyperfine constant for the state labeled by J. Because of the $\Delta M_I = 0$ selection rule the effect of the magnetic hyperfine interaction is to split each Zeeman component of a transition into 2I + 1 equally spaced lines. This can be expressed in frequency space as

$$\begin{aligned} \Delta\nu_{hf} &= M_I\ M_J"(a_J' - a_J") && \Delta M_J = 0 \\ &= M_I[(a_J' - a_J")\ M_J" \pm a'] && \Delta M_J = \pm 1 \end{aligned} \tag{8}$$

To transform these expressions into magnetic field space, we multiply by the term $(\partial H/d\nu)$. Note that we desire the shift in the field corresponding to a shift in the zero-field frequency ν_0 (not ν_L) caused by the hyperfine interactions. This derivative has the opposite sign of that of field with respect to ν_L. The result is

$$\Delta H_{hf} = \frac{M_I(a_J' - a_J'')(-1)}{\mu_0(g' - g'')} \qquad \Delta M_J = 0$$

$$= \frac{M_I[(a_J' - a_J'')\, M_J'' \pm a_J](-1)}{\mu_0(g' - g'')\, M_J'' \pm \mu_0 g'} \qquad \Delta M_J = +1 \qquad (9)$$

The form of the magnetic hyperfine coupling constant a_J can be obtained easily from the theory of gas phase electron resonance spectroscopy, so nicely worked out by Carrington and co-workers [27] a decade ago. For terms diagonal in all quantum numbers, the magnetic hyperfine constant for a Case A $^2\Pi$ state can be expressed as

$$a_J = \frac{\Omega h}{J(J + 1)} \qquad (10)$$

where $h = a + \Sigma(b + c)$, and a, b, and c are the Frosch and Foley hyperfine interaction constants, defined as reduced matrix elements over the unpaired electron density. From (9) we see that the shift in magnetic field due to the magnetic hyperfine interaction in a $\Delta M_J = 0$ spectrum is independent of M_J, and thus the hyperfine splitting is also independent of M_J in this case. For a $\Delta M_J = \pm 1$ spectrum that is not generally the case. Also, we note that for a positive h, $(a_J' - a_J'')$ is negative for $\Delta J = +1$ transitions with no change in Ω (pure rotational transitions). Since $(g_J' - g_J'')$ is also negative for these cases, the sign of the shift in the resonant field position caused by the magnetic hyperfine effect depends only on the sign of M_I for $\Delta M_J = 0$. For $\Delta M_J = \pm 1$ this is not generally true, and we must consider each specific case. However, it is usually true that for the fastest tuning transitions, the sign of M_J'' and the $\pm$ in (9) are correlated such that for a positive h the $+M_I$ component always appears at lowest field in both $\Delta M_J = 0$ and $\Delta M_J = +1$ transitions, at least in the situations we are considering. In summary, the appearance of magnetic hyperfine structure in the pure rotational LMR spectrum of a $^2\Pi_{3/2}$ molecule will be that of $(2I + 1)$ equally spaced, equally intense lines, with the $+M_I$ transitions appearing first in the low-field M_J components.

The presence of a nuclear electric quadrupole moment will destroy the equal spacing of hyperfine lines. The first-order

quadrupole energy in a decoupled basis can be expressed as

$$E_Q = Q_J[3M_J^2 - J(J+1)][3M_I^2 - I(I+1)] \qquad (11)$$

where

$$Q_J = \frac{eqQ}{4} \frac{[3\Omega^2 - J(J+1)]}{\{(2J-1)\,J(J+1)(2J+1)[3I - I(I+1)]\}}$$

Although this expression does not simplify as nicely as that for the magnetic hyperfine, we can still draw some useful generalizations from it. Because of the squared dependence on M_I the quadrupole interaction will cause the otherwise equally-spaced hyperfine levels to "bunch up"; that is, the spacing will either increase or decrease from lower to higher energies. The essentially $1/J^4$ dependence of Q_J causes the lower J state of the transition to dominate this effect in the transition. From (7) we noted that the order of the M_I states is opposite in Zeeman levels with opposite sign of M_J. This fact, together with the squared dependence on M_J in (11) means that the "bunching" of levels will occur in the same direction (from low to high energy or vice versa) in a $+M_J$ state as that in a $-M_J$ state. Therefore, whether the laser is above or below the zero field transition frequency will reverse the appearance of the hyperfine pattern. This is very similar to EPR patterns, which are reversed with a sign change in M_J. The pattern will depend only on the sign and magnitude of Q_J. We can deduce that for positive Q_J the hyperfine lines will converge to low fields when $\nu_L > \nu_0$, and if Q_J is negative or if $\nu_L < \nu_0$ they converge to high fields, for $|M_J| = J$.

Next we will consider the lambda doubling. At this stage we only want to determine how to assign the parity correctly. The lowest energy Krönig symmetry will generally be that which is the same as the lowest $^2\Sigma$ state, which will dominate the lambda doubling perturbation, e.g., if the lowest $^2\Sigma$ state has + Krönig symmetry, then + symmetry levels of the $^2\Pi$ state will be lower than - levels. We must then multiply the Krönig symmetry by the rotational phase factor $(-1)^{J-S}$ to get total parity. Therefore, for the usual case of a $^2\Sigma^+$ perturber, we have + parity the lowest for J = 1/2, - the lowest for J = 3/2, + the lowest for J = 5/2, and so on. In the $\Omega = 3/2$ state, lambda doubling increases with J. Therefore the <u>upper</u> state of a transition will determine the relative parity of the lambda-doubling components. Very simply, in a $J = 3/2 \rightarrow 5/2$ transition under the above conditions, the $- \rightarrow +$ parity component occurs at lower energy than the $+ \rightarrow -$ (parity must change in electric dipole transitions, of course). Therefore if the laser is at a lower frequency than the zero field rotational frequency, the $- \rightarrow +$ transition will appear at the lower

magnetic field, and vice-versa.

Finally, we shall discuss the very simple case of having different isotopic masses for a given molecule. Different masses will, of course, produce different rotational constants and hence different rotational energies. For light molecules (CH, OH, etc.) the isotope shift in the energies is large, such that different isotopes don't generally appear in the same spectrum, except through coincidence. For heavier molecules, the isotope shift may be small enough so that several species can be observed simultaneously. Then if the laser is above the zero-field transition frequency, the lighter isotopes appear at lowest fields; if ν_L is below ν_0, then the heavier isotopes appear first.

With only these simple ideas, an LMR spectrum can usually be assigned. The next step was to carry out a nonlinear least squares fit of the transition using a far more exact Hamiltonian. Again, most of the theory required to analyze LMR spectra was worked out earlier by Carrington, Levy, and Miller [28]. J. M. Brown [29] has since developed a more precise Zeeman Hamiltonian, and we have adopted his approach for $^2\Pi$ molecules. The detailed effective Hamiltonian used is given in almost complete form by Brown et al in [29], and we will not reproduce it here. The quadrupole interaction was not included in that work, however, and we have used the expressions from [28], to obtain its matrix elements in a decoupled Case A representation. The form of the effective $^2\Pi$ Hamiltonian used is

$$H_{eff} = H_{so} + H_{rot} + H_{cd} + H_{sr} + H_{LD} + H_{cdLD} + H_{hfs} + H_{cdhfs} + H_z \qquad (12)$$

where H_{so} represents spin-orbit coupling, H_{rot} and H_{cd} represent the rotational kinetic energy and centrifugal distortion, H_{sr} is the electron spin-rotation interaction, H_{LD} and H_{cdLD} represent the lambda doubling interaction and its centrifugal distortion corrections, H_{hfs} and H_{cdhfs} are the hyperfine interactions and distortion corrections, and H_z is the Zeeman interaction.

A computer program was written to set up the matrix elements of (12) including terms off-diagonal by ± 1 unit in J. For HBr^+ the matrices are 24 x 24 for each M_J value. Each M_J matrix is diagonalized and sorted at the appropriate resonant field position, differences are taken and the frequencies for each transition are then computed; the parameters are then iteratively adjusted until these transition frequencies converge to within some tolerance of the laser frequency. The size and structure of the data set dictates which of the parameters can be determined by this method.

INTERPRETATION OF MOLECULAR PARAMETERS IN TERMS OF ELECTRONIC STRUCTURE

Once a LMR spectrum has been detected, measured, and assigned, and the parameters extracted from a suitable analysis (such as a nonlinear regression method), the parameters are interpreted in terms of various integrals over the electronic distribution of the molecule. This subject has been developed to a high degree of sophistication for the purpose of analyzing microwave and electron paramagnetic resonance spectra [27,28,30]. We will review some of the salient aspects very briefly, but we do not present a detailed set of results for HBr^+ because our analysis is still in a very preliminary stage.

From a pure rotational LMR spectrum we can directly obtain the rotational constants, centrifugal distortion constants, hyperfine constants, lambda doubling constants, electron spin-rotation constants, quadrupole coupling parameters. In addition, measurement of cross-spin transitions ($\Delta\Omega \neq 0$) will directly measure the spin-orbit parameter and the spin-spin parameter for states with $S \geq 1$. If the data are precise enough, higher-order corrections to the g-factors that occur in the Zeeman Hamiltonian can be determined.

Once these parameters are determined, details of the electronic structure are revealed from their definitions as integrals over the electronic distributions. The rotational constants are the reciprocals of the moments of inertia averaged over the vibrational motion in the state they are measured for. The quantities of fundamental interest are not these effective rotational constants, but rather the equilibrium values, from which one can deduce the equilibrium structure of the molecule. This is possible only when rotational transitions have been measured in at least one excited level of every vibrational mode, which is usually not possible. One is thus generally forced to use the effective moments of inertia as an approximation to the equilibrium values. While the structure problem seems totally trivial for a diatomic molecule, the measurement of four isotopes of HBr^+ allows a rather precise determination of the bond distance through the use of Kraitchman's equations [31]. For a linear molecule this reduces to

$$|Z| = [\mu^{-1}(I_x' - I_x)]^{1/2} \tag{13}$$

where Z is the center-of-mass coordinate for the isotopically substituted atom, and I' and I are moments of inertia of the substituted and original molecules. Because we have measured two isotopes of both bromine and hydrogen, subtraction of the coordinates obtained from (13) will yield a precise approximation for

the equilibrium bond distance, in which the effect of the vibrational averaging has been largely eliminated. In general, LMR has the same capability as microwave spectroscopy for obtaining these precise substitution geometries for small molecules.

The magnetic hyperfine parameter h used in (10) is defined as

$$h = a + \Sigma(b + c) \tag{14}$$

The Frosch and Foley hyperfine constants a, b, and c are in turn defined as follows [30].

$$a = 2g_I \mu_N \mu_0 \left\langle \frac{1}{r^3} \right\rangle \text{ nuclear spin-electron orbit}$$

$$b + \frac{c}{3} = \frac{16\pi}{3} g_I \mu_N \mu_0 \Psi^2(0) \text{ Fermi contact}$$

$$c = 3g_i \mu_N \mu_0 \left\langle \frac{3\cos^2\theta - 1}{r^3} \right\rangle \text{ nuclear spin-electron spin} \tag{15}$$

In addition there is the parity-dependent spin-spin parameter

$$d = 3g_I \mu_N \mu_0 \left\langle \frac{\sin^2\theta}{r^3} \right\rangle$$

In these expressions r is the distance between the nucleus and the electrons and the average is over the unpaired electron density. If one can determine all of these integrals, then a detailed view of the unpaired electron distribution can be obtained. For example, the value of $\Psi^2(0)$ is non-negligible only for electrons in s orbitals, while a will be appreciable only for orbitals with non-zero orbital angular momentum, and c will similarly vanish for a spherical (s) orbital. By comparing values of $\langle 1/r^3 \rangle$, $\Psi^2(0)$,

$$\left\langle \frac{3\cos^2\theta - 1}{r^3} \right\rangle \text{ and } \left\langle \frac{\sin^2\theta}{r^3} \right\rangle$$

obtained from spectroscopic measurements of a, b, c, and d with values obtained for the free atoms, one can deduce the degree of atomic orbital (s, p, ...) character for a given open-shell molecular orbital system, and from this draw qualitative conclusions regarding the nature of the chemical bonding (double bond character, etc.) in the molecule.

The quadrupole coupling constant eqQ, provides similar but complementary information on the electronic structure. In this

constant, e is the nuclear charge and Q is the nuclear quadrupole moment, while $q = \langle \partial^2 V/\partial Z^2 \rangle$ is the field gradient at the nucleus, which can be expressed as

$$q = e\left\langle \frac{3\cos^2\theta - 1}{r^3} \right\rangle \tag{16}$$

The average in this expression is to be taken over the entire electron distribution, not just over the unpaired electron density. Evaluation of q can provide considerable insight as to the degree of ionic character of a bond, the amount of mixing of s and p atomic orbitals in a given molecular orbital, and also about the amount of multiple bond character.

We have shown that far-infrared laser magnetic resonance spectroscopy is a powerful new method for studying molecular ion structures. While our results for HBr^+ are most encouraging with respect to prospects for expanding the study to other charged species we should remind ourselves that these were a series of very difficult experiments. There are other promising candidates for LMR studies, including diatomics, like HCl^+, HF^+, HI^+, OH^+, NH^+, O_2^+, SH^+, PH^+, and polyatomics like H_2O^+, H_2S^+, NNO^+, and OCS^+; however, we should not expect any of these to be much easier to observe than HBr^+. Spectra, and the resulting determination of geometrical and electronic structures of other ions are very likely to proceed from LMR studies in the future, but each is guaranteed to contribute a certain amount of gray hair to the experimenters who do them.

ACKNOWLEDGMENT

The experimental part of this work was done at the National Bureau of Standards in Boulder, Colorado. R. J. S. thanks the National Research Council for a post-doctoral fellowship during that time (1977-79). The analysis of the HBr^+ spectra is being carried out at the University of California, Berkeley, by K. G. Lubic, who thanks the University for a Regents Fellowship (1980) and R. J. Saykally. R. J. S. and K. G. L. gratefully acknowledge support from the National Science Foundation grant CHE80-07042.

REFERENCES

1. G. H. Herzberg, Spectra and structures of molecular ions, in Quarterly Reviews (The Chemical Society, London, 1971), p. 201.
2. K. B. Jefferts, Phys. Rev. Lett. 20, 39 (1968); 23, 1476 (1969).

3. D. Buhl and L. E. Snyder, Nature 228, 267 (1970).
4. B. E. Turner, App. J. 193, L83 (1974).
5. T. A. Dixon and R. C. Woods, Phys. Rev. Lett. 34, 61 (1975).
6. R. C. Woods, T. A. Dixon, R. J. Saykally, and P. G. Szanto, Phys. Rev. Lett. 35, 1269 (1975).
7. R. J. Saykally, T. A. Dixon, T. G. Anderson, P. G. Szanto, and R. C. Woods, App. J. 205, L101 (1976).
8. W. H. Wing, G. A. Ruff, W. E. Lamb, and J. J. Spezeski, Phys. Rev. Lett. 36, 1488 (1976).
9. D. E. Tolliver, G. A. Kyrala, W. H. Wing, Phys. Rev. Lett. 43, 1719 (1979).
10. J. T. Shy, J. W. Farley, W. E. Lamb, Jr., and W. H. Wing, Phys. Rev. Lett. 45, 535 (1980).
11. A. Carrington, P. L. Milverton, and P. G. Sarre, Mol. Phys. 35, 1505 (1978).
12. A. Carrington, P. L. Milverton, P. G. Roberts, and P. J. Sarre, J. Chem. Phys. 68, 5659 (1978).
13. A. Carrington, P. G. Roberts, and P. J. Sarre, Mol. Phys. 35, 1523 (1978).
14. M. Tadjeddine, R. Abouaf, P. C. Cosby, B. A. Huber, and J. T. Moseley, J. Chem. Phys. 69, 710 (1978); J. T. Moseley, P. C. Cosby, J. B. Ozenne, and J. Durup, J. Chem. Phys. 70, 1474 (1979).
15. A. Carrington, private communication (1980).
16. R. J. Saykally and K. M. Evenson, Phys. Rev. Lett. 43, 515 (1979).
17. T. Oka, Phys. Rev. Lett. 45, 531 (1980).
18. F. Grieman, Ph.D. Thesis, University of California, Berkeley, CA and F. J. Grieman, B. H. Mahan, A. O'Keefe, and J. S. Winn, to be published.
19. K. M. Evenson, R. J. Saykally, D. A. Jennings, R. F. Curl, Jr., and J. M. Brown, Far infrared laser magnetic resonance, in: "Chemical and Biochemical Applications of Lasers", Vol. V, C. B. Moore, ed., Academic Press, New York (1980).
20. R. J. Saykally and K. M. Evenson, J. Chem. Phys. 71, 1564 (1979).
21. A. Scalabrin, R. J. Saykally, K. M. Evenson, H. E. Radford, and M. Mizushima, J. Mol. Spectrom. (to be published).
22. R. J. Saykally and K. M. Evenson, J. Chem. Phys. (to be published).
23. R. J. Saykally, Ph.D. Thesis, University of Wisconsin, Madison, WI (1977).
24. K. L. Saenger, R. N. Zare, and C. W. Mathews, J. Mol. Spectrom. 61, 216 (1976).
25. F. C. Fehsenfeld and E. E. Fergeson, J. Chem. Phys. 60, 5132 (1974).
26. R. F. Barrow and A. D. Caunt, Proc. Phys. Soc. A66, 617 (1953).
27. A. Carrington, "Microwave Spectroscopy of Free Radicals," Academic Press, New York (1974).

28. A. Carrington, D. H. Levy, and T. A. Miller, Adv. Chem. Phys. 18, 149 (1970).
29. J. M. Brown, M. Kaise, C. M. L. Kerr, and D. J. Milton. Mol. Phys. 36, 553 (1978).
30. C. H. Townes and A. L. Schawlow, "Microwave Spectroscopy," Dover, Inc., New York (1975).
31. J. Kraitchman, Am. J. Phys. 21, 17 (1953).